

---

# FDTD Simulation von Elektronenstreuung an einer elektromagnetischen Welle

## FDTD Simulation of electron scattering in an electromagnetic wave

David Symhoven

---



München 2017



---

# FDTD Simulation von Elektronenstreuung an einer elektromagnetischen Welle

## FDTD Simulation of electron scattering in an electromagnetic wave

David Symhoven

---

Masterarbeit  
am Lehrstuhl Computational & Plasma Physics  
der Ludwig-Maximilians-Universität  
München

vorgelegt von  
David Symhoven  
aus Witten

München, den 18.07.2017

Erstgutachter: Prof.Dr.Hartmut Ruhl  
Zweitgutachter: Zweitgutachter

---

## Introduction

---

Now it's going loose ...<sup>[1]</sup>  
What is the goal of this thesis?  
What is Plasma, and where is it used ?  
Summary of all chapters

---

## Symbols and Constants

---

Vacuum permittivity	$\epsilon_0$	$8.85418781762 \cdot 10^{-12} \text{ A s V}^{-1} \text{ m}^{-1}$
Vacuum permeability	$\mu_0$	$2566370614 \cdot 10^{-6} \text{ N A}^{-2}$
Speed of Light	$c$	$299792458 \text{ m s}^{-1}$
Electrical flux density	$\vec{D}$	$[\text{A s m}^{-2}]$
Magnetic flux density	$\vec{B}$	$[\text{T}]$
Magnetic field strength	$\vec{H}$	$[\text{A m}^{-1}]$
Electric field strength	$\vec{E}$	$[\text{V m}^{-1}]$
Poynting Vector	$\vec{S}$	$[\text{N m}^{-1} \text{ s}^{-1}]$
Nabla - Operator	$\vec{\nabla}$	$\left( \frac{\partial}{\partial r_1}, \dots, \frac{\partial}{\partial r_n} \right)$
Laplace - Operator	$\Delta$	$\sum_{i=1}^n \frac{\partial^2}{\partial r_i^2}$
d'Alembert - Operator	$\hat{\square}$	$\Delta - \frac{1}{c^2} \frac{\partial^2}{\partial t^2}$

---

## Contents

---

<b>I. Fundamentals</b>	<b>2</b>
<b>1. Electromagnetic radiation</b>	<b>3</b>
1.1. Maxwell-Equations . . . . .	3
1.2. Colomb and Lorentz Gauge . . . . .	4
1.3. Liénard-Wiechert Potentials . . . . .	5
1.3.1. Solution of inhomogeneous wave equation . . . . .	5
1.3.2. Special Case: Moving point charge . . . . .	7
1.3.3. Energy emission . . . . .	9
<b>II. Numerics</b>	<b>14</b>
<b>2. Integration of Equation of Motion</b>	<b>16</b>
2.1. Equations of Motion . . . . .	16
2.2. Euler-Scheme . . . . .	16
2.2.1. Procedural Error and Order of Consistency . . . . .	18
2.3. Leap-Frog-Scheme . . . . .	19
2.3.1. Boris-Method . . . . .	20
2.4. Nyström-Scheme . . . . .	22
2.5. Adaptive Timestep Control . . . . .	22
<b>3. Interpolations</b>	<b>23</b>
3.1. Linear interpolation of Trajectories . . . . .	23
3.2. Trilinear Interpolation of Fields . . . . .	25
<b>4. FDTD</b>	<b>26</b>
4.1. Maxwell-Equations . . . . .	26
4.2. The Yee-Scheme . . . . .	27
4.3. Numeric Dispersion Relation . . . . .	28

## CONTENTS

---

<b>5. Hybrid Field Approach</b>	<b>29</b>
5.1. Near-and Farfields . . . . .	29
5.2. Particle Push and Nearfield Update . . . . .	29
5.3. Particle History . . . . .	29
5.4. Farfield Setup Before Simulation . . . . .	29
5.5. Electron Scattering in an electromagnetic wave . . . . .	29
<b>6. Uniaxial Perfectly Matched Layer</b>	<b>30</b>
 <b>III. Summary</b>	 <b>31</b>
 <b>IV. Appendix</b>	 <b>32</b>
<b>A. Gauge Transformations</b>	<b>33</b>
A.1. Invariance of Fields . . . . .	33
A.2. Invariance of Potential Equations . . . . .	34
<b>B. Retarded Potential Equations Fulfill Laurentz Gauge</b>	<b>35</b>
<b>C. Softwarestack</b>	<b>37</b>
<b>D. Code Documentation</b>	<b>38</b>
<b>E. Normalization</b>	<b>39</b>
<b>Bibliography</b>	<b>41</b>
<b>Declaration</b>	<b>42</b>



Part I.

# Fundamentals

---

## Electromagnetic radiation

---

In the first section we want to talk about electromagnetic radiation.

### 1.1 Maxwell-Equations

The Maxwell equations are the foundation of the classical electromagnetism and describe how the electric field strength  $\vec{E} \in \mathbb{R}^3$  and the magnetic field strength  $\vec{H} \in \mathbb{R}^3$  are generated by charges and currents respectively and how they evolve over time in space in presence of one another. In presence of matter however, the interaction of the fields with the material need to be taken into account. The effect of microscopic dipoles, formed by bound charge carriers, are summarized in macroscopic entities called Polarisation  $\vec{P} \in \mathbb{R}^3$  and Magnetization  $\vec{M} \in \mathbb{R}^3$ . These dipoles align in the external field such that the resulting electric and magnetic field are described by

$$\begin{aligned}\vec{D} &:= \epsilon_0 \vec{E} + \vec{P} \\ \vec{H} &:= \frac{1}{\mu_0} \vec{B} - \vec{M},\end{aligned}\tag{1.1}$$

where  $\mu_0$  and  $\epsilon_0$  are the vacuum permeability and permittivity respectively. The macroscopic Maxwell Equations than read

$$\vec{\nabla} \cdot \vec{B} = 0 \tag{1.2}$$

$$\vec{\nabla} \cdot \vec{D} = \rho \tag{1.3}$$

$$\vec{\nabla} \times \vec{E} = -\frac{\partial \vec{B}}{\partial t} \tag{1.4}$$

$$\vec{\nabla} \times \vec{H} = \frac{\partial \vec{D}}{\partial t} + \vec{j}, \tag{1.5}$$

where  $\rho$  denotes the charge density of the electric source and  $\vec{j}$  the electric current density. In the case of vacuum, the material equations (1.6) reduce to

$$\begin{aligned}\vec{D} &= \epsilon_0 \vec{E} \\ \vec{H} &= \frac{1}{\mu_0} \vec{B}.\end{aligned}\tag{1.6}$$

## 1.2 Colomb and Lorentz Gauge

In the following section we consider the Maxwell Equations in vacuum.

The electric and magnetic fields can also be described by a scalar and a vector potential respectively. From (1.2) we can conclude that

$$\exists \vec{A} \in \mathbb{R}^3: \vec{B} = \vec{\nabla} \times \vec{A},\tag{1.7}$$

where  $\vec{A}$  is called the vector potential. Plugging in (1.7) into (1.4) yields

$$\begin{aligned}\vec{\nabla} \times \left( \vec{E} + \frac{\partial \vec{A}}{\partial t} \right) &= 0. \\ \Rightarrow \exists \varphi \in \mathbb{R}: \vec{E} + \frac{\partial \vec{A}}{\partial t} &= -\vec{\nabla} \varphi.\end{aligned}\tag{1.8}$$

$\varphi$  is called scalar potential. Plugging in (1.8) into (1.3) and also (1.7) and (1.8) into (1.5) gives the potential equations

$$\begin{aligned}-\Delta \varphi - \vec{\nabla} \left( \frac{\partial \vec{A}}{\partial t} \right) &= \frac{\rho}{\epsilon_0} \\ \underbrace{\left( \Delta - \frac{1}{c^2} \frac{\partial^2}{\partial t^2} \right)}_{:= \hat{\Box}} \vec{A} - \vec{\nabla} \left( \vec{\nabla} \vec{A} + \frac{1}{c^2} \frac{\partial \varphi}{\partial t} \right) &= -\mu_0 \vec{j},\end{aligned}\tag{1.9}$$

where we used the *Graßmann Identity*:  $\vec{\nabla} \times (\vec{\nabla} \times \vec{A}) = \vec{\nabla}(\vec{\nabla} \vec{A}) - \Delta \vec{A}$ .

The description of the fields by the aforementioned potentials  $\varphi$  and  $\vec{A}$  are not unique. This is called gauge freedom. The potentials can be specifically adjusted to the problem at hand. The gauge transformations look like

$$\begin{aligned}\vec{A} &\mapsto \vec{A}' = \vec{A} + \vec{\nabla} \psi \\ \varphi &\mapsto \varphi' = \varphi - \frac{\partial \psi}{\partial t},\end{aligned}\tag{1.10}$$

where  $\psi: \mathbb{R}^3 \times \mathbb{R} \mapsto \mathbb{R}$ . In appendix A we show, that  $\psi$  does indeed not change the physics.

If we choose  $\psi$  such that

$$\vec{\nabla} \vec{A} + \frac{1}{c^2} \frac{\partial \varphi}{\partial t} = 0, \quad (1.11)$$

then we call it a *Lorentz Gauge* and the potential Equations (1.9) decouple into two separate wave equations

$$\begin{aligned} \hat{\square} \varphi &= -\frac{\rho}{\epsilon_0} \\ \hat{\square} \vec{A} &= -\mu_0 \vec{j}. \end{aligned} \quad (1.12)$$

### 1.3 Liénard-Wiechert Potentials

#### 1.3.1 Solution of inhomogeneous wave equation

The *Liénard-Wiechert* Potentials are the solution of (1.12). Following<sup>[5]</sup> we solve the general case

$$\hat{\square} \psi(\vec{r}, t) = f(\vec{r}, t), \quad (1.13)$$

where  $\psi, f: \mathbb{R}^3 \times \mathbb{R} \mapsto \mathbb{R}$ .  $f$  is called source function and will be specified later. (1.13) is a linear inhomogeneous partial differential equation. Those kind of equations are solved with the *Green's function* approach. If we can find the Green's function  $G$  fulfilling

$$\hat{\square} G(\vec{r} - \vec{r}', t - t') = -\delta(\vec{r} - \vec{r}') \delta(t - t'), \quad (1.14)$$

then we can calculate the solution of (1.13) via

$$\psi(\vec{r}, t) = \int \int G(\vec{r} - \vec{r}', t - t') f(\vec{r}', t') dt' d\vec{r}'. \quad (1.15)$$

To find  $G$  we use the following Fourier - Transformations

$$\begin{aligned} G(\vec{r} - \vec{r}', t - t') &= \frac{1}{4\pi^2} \int \int G(\vec{k}, \omega) \exp(i\vec{k}(\vec{r} - \vec{r}')) \exp(-i\omega(t - t')) d\omega d\vec{k}, \\ \delta(\vec{r} - \vec{r}') &= \frac{1}{4\pi^2} \int \exp(i\vec{k}(\vec{r} - \vec{r}')) d\vec{k}, \\ \delta(t - t') &= \frac{1}{4\pi^2} \int \exp(-i\omega(t - t')) d\omega. \end{aligned} \quad (1.16)$$

Plugging in (1.16) into (1.14) yields

$$\int \int \exp(i\vec{k}(\vec{r} - \vec{r}')) \exp(-i\omega(t - t')) \left[ G(\vec{k}, \omega) \left( -k^2 + \frac{\omega^2}{c^2} \right) + \frac{1}{4\pi^2} \right] = 0,$$

which leaves us with

$$G(\vec{k}, \omega) = \frac{1}{4\pi^2} \frac{1}{k^2 - \frac{\omega^2}{c^2}}.$$

Using residue theorem we find the Fourier Back Transform of G to be

$$G_{ret}(\vec{r} - \vec{r}', t - t') = \frac{\delta(t' - t_{ret})}{4\pi|\vec{r} - \vec{r}'|}, \quad (1.17)$$

where

$$t_{ret} := t - \frac{|\vec{r} - \vec{r}'|}{c} \quad (1.18)$$

is the retarded time. We also call  $G_{ret}$  the *retarded Green's function* in contrast to the *advanced Green's function*  $G_{av}$  with the advanced time

$$t_{av} := t + \frac{|\vec{r} - \vec{r}'|}{c}. \quad (1.19)$$

The latter does not fulfill the causal principle of physics. We expect the reason for a change in our signal at  $\vec{r}$  at time  $t$ , due to a perturbation, to be in the past, not the future. Because  $t_{ret} < t$  the retarded Green's function is the one to work with. Plugging in (1.17) into (1.15) yields

$$\psi(\vec{r}, t) = \frac{1}{4\pi} \int \frac{f(\vec{r}', t_{ret})}{|\vec{r} - \vec{r}'|} d\vec{r}', \quad (1.20)$$

which finally leads to the retarded potential equations

$$\varphi(\vec{r}, t) = \frac{1}{4\pi\epsilon_0} \int \frac{\rho(\vec{r}', t_{ret})}{|\vec{r} - \vec{r}'|} d\vec{r}', \quad (1.21)$$

$$\vec{A}(\vec{r}, t) = \frac{\mu_0}{4\pi} \int \frac{\vec{j}(\vec{r}', t_{ret})}{|\vec{r} - \vec{r}'|} d\vec{r}'. \quad (1.22)$$

Lastly we show in Appendix B that they indeed fulfill the Laurentz Gauge (1.11).

### 1.3.2 Special Case: Moving point charge

Now we want to discuss the special case of a particle with charge  $q$ , moving along the trajectory  $\vec{r}_p$  with velocity  $\vec{v} := \dot{\vec{r}}_p$ , where the dot donates the time derivative. As mentioned before, we now define the source functions for our problem at hand. For the charge density we have

$$\rho(\vec{r}, t) = q\delta(\vec{r} - \vec{r}_p(t)) \quad (1.23)$$

and for the current density

$$\vec{j}(\vec{r}, t) = q\vec{v}\delta(\vec{r} - \vec{r}_p(t)). \quad (1.24)$$

Identifying

$$\begin{aligned} \psi(\vec{r}, t) &= \varphi(\vec{r}, t) \text{ and } f(\vec{r}', t') = \frac{\rho(\vec{r}', t')}{\epsilon_0}, \\ \vec{\psi}(\vec{r}, t) &= \vec{A}(\vec{r}, t) \text{ and } \vec{f}(\vec{r}', t') = \mu_0 \vec{j}(\vec{r}', t') \end{aligned}$$

and using (1.15) with (1.17) yields after integrating over  $\vec{r}'$

$$\begin{aligned} \varphi(\vec{r}, t) &= \frac{1}{4\pi\epsilon_0} \int \frac{\delta\left(\frac{|\vec{r}-\vec{r}_p|}{c} - t + t'\right)}{|\vec{r} - \vec{r}_p|} dt', \\ \vec{A}(\vec{r}, t) &= \frac{q\mu_0}{4\pi} \int \vec{v}(t') \frac{\delta\left(\frac{|\vec{r}-\vec{r}_p|}{c} - t + t'\right)}{|\vec{r} - \vec{r}_p|} dt'. \end{aligned} \quad (1.25)$$

For the  $t'$  - integration we need the following property of the  $\delta$  - distribution

$$\delta[g(t')] = \sum_{i=1}^n \frac{\delta(t' - t_i)}{\left|\left(\frac{dg}{dt'}\right)\right|_{t'=t_i}}, \quad (1.26)$$

where

$$g(t') := \frac{|\vec{r} - \vec{r}_p|}{c} - t + t' \quad (1.27)$$

and  $t_i$  are the roots of  $g$ . To find the roots of  $g$ , let's consider

$$\begin{aligned} \frac{dg}{dt'} &= 1 + \frac{1}{c} \frac{d}{dt'} |\vec{r} - \vec{r}_p| = 1 - \frac{\vec{v}(t')}{c} \underbrace{\frac{\vec{r} - \vec{r}_p}{|\vec{r} - \vec{r}_p|}}_{|\cdot|=1} \\ \implies 1 - \frac{\vec{v}(t')}{c} &\leq \frac{dg}{dt'} \leq 1 + \frac{\vec{v}(t')}{c} \\ \xrightarrow{v \leq c} \frac{dg}{dt'} &> 0, \end{aligned} \tag{1.28}$$

which means that  $g$  is a monotonically increasing function and therefore has at most one root, which is  $t' = t_{ret}$  as can be seen from (1.27). In case that  $g$  has no roots at all, we can conclude that  $\varphi \equiv 0$  and  $\vec{A} \equiv 0$ .

With  $t_{ret} := t - \frac{|\vec{r} - \vec{r}_p|}{c}$  the integration over  $t'$  yields

$$\begin{aligned} \varphi(\vec{r}, t) &= \frac{1}{4\pi\epsilon_0} \frac{q}{|\vec{r} - \vec{r}_p(t_{ret})| - \frac{\vec{v}(t_{ret})}{c} (\vec{r} - \vec{r}_p(t_{ret}))}, \\ \vec{A}(\vec{r}, t) &= \frac{1\mu_0}{4\pi} \frac{q\vec{v}(t_{ret})}{|\vec{r} - \vec{r}_p(t_{ret})| - \frac{\vec{v}(t_{ret})}{c} (\vec{r} - \vec{r}_p(t_{ret}))} \end{aligned} \tag{1.29}$$

which are the *Liénard-Wiechert* Potentials. Upon defining

$$\begin{aligned} \vec{\beta}(t) &:= \frac{\vec{v}(t)}{c}, \\ \vec{R}(\vec{r}, t) &:= \vec{r} - \vec{r}_p(t), \\ \vec{n}(\vec{r}, t) &:= \frac{\vec{R}(\vec{r}, t)}{R(\vec{r}, t)} \end{aligned} \tag{1.30}$$

we can rewrite the Liénard-Wiechert Potentials in a more compact and final form

$$\begin{aligned} \varphi(\vec{r}, t) &= \frac{1}{4\pi\epsilon_0} \frac{q}{(1 - \vec{\beta}(t') \cdot \vec{n}(\vec{r}, t')) R(\vec{r}, t')} \Big|_{t'=t_{ret}}, \\ \vec{A}(\vec{r}, t) &= \frac{\mu_0}{4\pi} \frac{q\vec{\beta}(t')}{(1 - \vec{\beta}(t') \cdot \vec{n}(\vec{r}, t')) R(\vec{r}, t')} \Big|_{t'=t_{ret}}. \end{aligned} \tag{1.31}$$

They are the generalization of the Coulomb Potential. With the help of (1.8) the electric and magnetic fields can be derived from the *Liénard-Wiechert* Potentials (1.31). Since

this is a quite longish calculation we refer to<sup>[5]</sup> and just present the final result

$$\begin{aligned}\vec{E}(\vec{r}, t) &= \frac{q}{4\pi\epsilon_0} \left( \frac{\vec{n}(\vec{r}, t') - \vec{\beta}(t)}{\gamma^2(1 - \vec{\beta}(t) \cdot \vec{n}(\vec{r}, t'))^3 R^2(\vec{r}, t')} \right. \\ &\quad \left. + \frac{1}{c} \frac{\vec{n}(\vec{r}, t') \times (\vec{n}(\vec{r}, t') - \vec{\beta}(t)) \times \dot{\vec{\beta}}(t)}{(1 - \vec{\beta}(t) \cdot \vec{n}(\vec{r}, t'))^3 R^2(\vec{r}, t')} \right) \Big|_{t'=t_{ret}}, \\ \vec{B}(\vec{r}, t) &= \frac{1}{c} \left( \vec{n}(\vec{r}, t') \times \vec{E}(\vec{r}, t) \right) \Big|_{t'=t_{ret}}.\end{aligned}\tag{1.32}$$

This is the electric and magnetic field of a moving charged particle. Due to the finite speed of light, the fields need time to travel from their source to the observation point. That means, that the fields at time  $t$ , were actually produced at a earlier time  $t_{ret}$ . As can be seen in figure 3.1, the retarded time is determined by the intersection point of the particle trajectory with the backward lightcone of the observation point.

### 1.3.3 Energy emission

Now we want to discuss the energy flow and emission. Therefore we need to analyze the Poynting Vector

$$\vec{S} = \frac{1}{\mu_0} \vec{E} \times \vec{B} = \frac{1}{\mu_0 c} \left[ \vec{n}_{ret} E^2 - \left( \vec{n}_{ret} \vec{E} \right) \cdot \vec{E} \right],\tag{1.33}$$

where  $\vec{n}_{ret} := \vec{n}(\vec{r}, t_{ret})$ . Taking a closer look at (1.32) reveals that both  $\vec{E}$  and  $\vec{B}$  can be separated into two parts, one of which is not dependent on the particle acceleration

$$\begin{aligned}\vec{E}_{(v)}(\vec{r}, t) &= \frac{q}{4\pi\epsilon_0} \frac{1}{\gamma^2(1 - \vec{\beta}(t') \cdot \vec{n}(\vec{r}, t'))^3 R^2(\vec{r}, t')} \left( \vec{n}(\vec{r}, t') - \vec{\beta}(t') \right) \Big|_{t'=t_{ret}} \\ \vec{B}_{(v)}(\vec{r}, t) &= \frac{q}{4\pi\epsilon_0 c} \frac{1}{\gamma^2(1 - \vec{\beta}(t') \cdot \vec{n}(\vec{r}, t'))^3 R^2(\vec{r}, t')} \underbrace{\left[ \vec{n} \times (\vec{n}(\vec{r}, t') - \vec{\beta}(t')) \right]}_{=\frac{1}{c}(\vec{v} \times \vec{n})} \Big|_{t'=t_{ret}}\end{aligned}\tag{1.34}$$



whilst the other is through  $\dot{\vec{\beta}}$

$$\begin{aligned}\vec{E}_{(a)}(\vec{r}, t) &= \frac{q}{4\pi\epsilon_0 c} \frac{\vec{n}(\vec{r}, t') \times \left( \vec{n}(\vec{r}, t') - \vec{\beta}(t') \right) \times \dot{\vec{\beta}}(t')}{\left( 1 - \vec{\beta}(t') \cdot \vec{n}(\vec{r}, t') \right)^3 R(\vec{r}, t')} \Big|_{t'=t_{ret}} \\ \vec{B}_{(a)}(\vec{r}, t) &= \frac{q}{4\pi\epsilon_0 c^2} \frac{\vec{n}(\vec{r}, t') \times \left[ \vec{n}(\vec{r}, t') \times \left( \vec{n}(\vec{r}, t') - \vec{\beta}(t') \right) \times \dot{\vec{\beta}}(t') \right]}{\left( 1 - \vec{\beta}(t') \cdot \vec{n}(\vec{r}, t') \right)^3 R(\vec{r}, t')} \Big|_{t'=t_{ret}}.\end{aligned}\tag{1.35}$$

Since  $E_{(v)} \propto \frac{1}{R^2}$  whereas  $E_{(a)} \propto \frac{1}{R}$ , its field contributions will dominate in the far field, i.e. for large distances from the source. Plugging in (1.32) in (1.33) gives us several terms with different orders of  $\frac{1}{R}$ , namely

$$\begin{aligned}\vec{S}_{vv} &\propto \left| \vec{E}_{(v)} \times \vec{B}_{(v)} \right| \propto \frac{1}{R^4}, \\ \vec{S}_{va} &\propto \left| \vec{E}_{(v)} \times \vec{B}_{(a)} \right| \propto \frac{1}{R^3}, \\ \vec{S}_{aa} &\propto \left| \vec{E}_{(a)} \times \vec{B}_{(a)} \right| \propto \frac{1}{R^2}.\end{aligned}$$

By evaluating the energy flux through an arbitrary surface with differential surface area  $d\vec{\sigma}$ , as illustrated in figure 1.1,

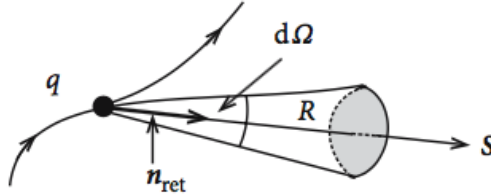


Figure 1.1.: Illustration of how to calculate the energy emission of a moving particle with charge  $q$ .<sup>[5]</sup>

we can see, that it will suffice to only consider the  $\frac{1}{R^2}$  terms, because the  $\frac{1}{R^3}$  or higher terms do not contribute to the energy emission, since

$$\oint \vec{S} d\vec{\sigma} \rightsquigarrow \oint \frac{1}{R^3} r^2 d\Omega \rightsquigarrow \oint \frac{1}{r} d\Omega \rightsquigarrow \frac{1}{r} \xrightarrow{r \rightarrow \infty} 0,\tag{1.36}$$

where  $d\Omega := \sin(\vartheta)d\vartheta d\varphi$ . That means we can focus on (1.35) when calculating (1.33)

$$\vec{S} = \frac{1}{\mu_0 c} \frac{q^2}{16\pi^2 \epsilon_0^2 c^2} \frac{\vec{n}(\vec{r}, t') \left[ \vec{n}(\vec{r}, t') \times \left( \vec{n}(\vec{r}, t') - \vec{\beta}(t') \right) \times \dot{\vec{\beta}}(t') \right]^2}{\left( 1 - \vec{\beta}(t') \cdot \vec{n}(\vec{r}, t') \right)^6 R^2(\vec{r}, t')} \Big|_{t'=t_{ret}} + \mathcal{O}\left(\frac{1}{R^3}\right) \quad (1.37)$$

The energy flux has the direction of  $\vec{n}_{ret}$ , i.e. it flows from the particle position  $\vec{r}_p$  at time  $t' = t_{ret}$  to the observation point  $\vec{r}$ . We can also see, that only accelerated particles ( $\dot{\vec{\beta}} \neq 0$ ) loose energy through radiation, which leads to a reduction in kinetic energy. Although an uniformly moving particle produces E and B - fields, it does not loose energy through radiation.

Lastly we want to discuss the radiation power. The emitted energy per time  $dt$  into the solid angle  $d\Omega$  is described by

$$\frac{dW}{d\Omega} = \left( \vec{S} \cdot \vec{n}(\vec{r}, t') \right) R^2(\vec{r}, t') \Big|_{t'=t_{ret}}. \quad (1.38)$$

Usually the observed amount of energy per unit time  $dt$  is not the same as the emitted energy of the particle per unit time  $dt_{ret}$ . To learn more about the emission within the particles system, we want to express our equation in terms of  $dt_{ret}$ , which gives us

$$\frac{dW}{d\Omega} = \left( \vec{S} \cdot \vec{n}(\vec{r}, t') \right) R^2(\vec{r}, t') \left( \frac{dt}{dt'} \right) \Big|_{t'=t_{ret}}. \quad (1.39)$$

From the definition of  $t_{ret} := t' - \frac{|\vec{r} - \vec{r}'|}{c}$  we find

$$\left( \frac{dt}{dt'} \right) \Big|_{t'=t_{ret}} = \left( 1 + \frac{1}{c} \frac{d}{dt'} |\vec{r} - \vec{r}_p(t')| \right) \Big|_{t'=t_{ret}} = \left( 1 - \frac{1}{c} \vec{n}(\vec{r}, t') \vec{v}(t') \right) \Big|_{t'=t_{ret}}. \quad (1.40)$$

Finally we obtain

$$\frac{dW}{d\Omega} = \frac{q^2}{16\pi^2 \epsilon_0 c} \frac{\left[ \vec{n}(\vec{r}, t') \times \left( \vec{n}(\vec{r}, t') - \vec{\beta}(t') \right) \times \dot{\vec{\beta}}(t') \right]^2}{\left( 1 - \vec{\beta}(t') \cdot \vec{n}(\vec{r}, t') \right)^5} \Big|_{t'=t_{ret}}. \quad (1.41)$$

Now we can discuss two cases. The non relativistic case ( $\beta \approx 0$ ) and the relativistic case ( $\beta \approx 1$ ).

$\beta \approx 0$ : In this case (1.41) simplifies to

$$\begin{aligned}
 \frac{dW}{d\Omega} &= \frac{q^2}{16\pi^2\epsilon_0 c} \left[ \vec{n}(\vec{r}, t') \times \left( \vec{n}(\vec{r}, t') \times \dot{\vec{\beta}}(t') \right) \right]^2 \Big|_{t'=t_{ret}} \\
 &= \frac{q^2}{16\pi^2\epsilon_0 c} \left[ \underbrace{\left( \vec{n}(\vec{r}, t') \cdot \dot{\vec{\beta}}(t') \right)}_{=\dot{\beta}n \cos(\vartheta)} \vec{n}(\vec{r}, t') - \underbrace{\left( \vec{n}(\vec{r}, t') \cdot \vec{n}(\vec{r}, t') \right)}_{|\cdot|=1} \dot{\vec{\beta}}(t') \right]^2 \Big|_{t'=t_{ret}} \\
 &= \frac{q^2 \dot{\beta}_{ret}^2}{16\pi^2\epsilon_0 c} (\cos^2(\vartheta) - 2\cos^2(\vartheta) + 1) \\
 &= \frac{q^2 \dot{\beta}_{ret}^2}{16\pi^2\epsilon_0 c} \sin^2(\vartheta),
 \end{aligned}$$

where  $\vartheta$  is the angle between  $\dot{\vec{\beta}}$  and  $\vec{n}$ .  $\beta_{ret}$  means again the evaluation at  $t' = t_{ret}$ . We conclude, that the direction of maximum radiation is perpendicular to the particles direction of motion, in contrast to

$\beta \approx 1$ : where we will see shortly, that the maximum radiation will be primarily in the direction of motion of the particle. We will restrict ourselves to the simple case, where  $\dot{\vec{\beta}} \parallel \vec{\beta}$ . Following the same steps as above we obtain

$$\frac{dW}{d\Omega} = \frac{q^2 \dot{\beta}_{ret}^2}{16\pi^2\epsilon_0 c} \frac{\sin^2(\vartheta)}{(1 - \beta(t') \cos(\vartheta))^5}. \quad (1.42)$$

To get the angle, where the radiation is maximal, we calculate

$$\begin{aligned}
 \frac{d}{d(\cos(\vartheta))} \left( \frac{dW}{d\Omega} \right) &\stackrel{!}{=} 0 \\
 \iff -2\cos(\vartheta) (1 - \beta_{ret} \cos(\vartheta))^5 + 5\beta_{ret}(1 - \cos^2(\vartheta)) (1 - \beta_{ret} \cos(\vartheta))^4 &\stackrel{!}{=} 0 \\
 \iff (1 - \beta_{ret} \cos(\vartheta))^4 [-2\cos(\vartheta) (1 - \beta_{ret} \cos(\vartheta)) + 5\beta_{ret}(1 - \cos^2(\vartheta))] &\stackrel{!}{=} 0 \\
 \implies -2\cos(\vartheta) (1 - \beta_{ret} \cos(\vartheta)) + 5\beta_{ret}(1 - \cos^2(\vartheta)) &\stackrel{!}{=} 0 \\
 \iff \cos^2(\vartheta) + \frac{2}{3\beta_{ret}} \cos(\vartheta) - \frac{5}{3} &\stackrel{!}{=} 0 \\
 \implies \cos(\vartheta)_{max} = \frac{1}{3\beta_{ret}} \left( \sqrt{1 + 15\beta_{ret}^2} - 1 \right).
 \end{aligned}$$

Obviously the angle decreases monotonically with increasing velocity, i.e. increasing  $\beta_{ret}$ . For  $\beta_{ret} = 1$  we get  $\cos(\vartheta) = 1$  or equivalently  $\vartheta = 0$ . In figure 1.2 the results are summarized.

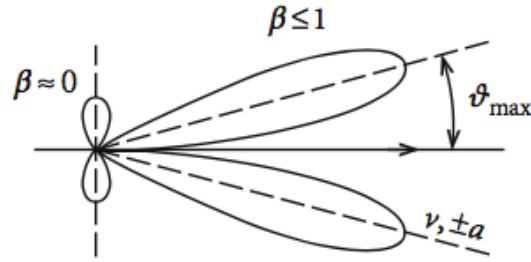


Figure 1.2.: Radiation characteristics of an moving charged particle.<sup>[5]</sup>

Part II.

Numerics

---

The following section deals with the numeric aspects of this thesis. We explain the underlying equation of motions and their history. After that, we go into several methods with which we can solve differential equations. Over the course of the last decades numerous methods were invented each of which has its own strength and weaknesses. Some of them are very easy to implement, which in turn usually leads to unprecise results. Others are quite complicated and sophisticated to implement, but very accurate. Therefore one should always consider which method is best for the problem and what it is one want to achieve.

Following this, we also want to define and calculate the numerical complexity of some chosen algorithms.

---

## Integration of Equation of Motion

---

### 2.1 Equations of Motion

As we know from mechanics the dynamic of a particle is determined by the forces acting on it. In our case there is a force due to electro-magnetic fields. That can be external fields, but also fields due to moving particles, as we explained in section 1.3.

The dynamics of our system is described by the *Lorentz-Newton* equation

$$\begin{aligned}\frac{dx^\mu}{d\tau} &= u^\mu \\ \frac{du^\mu}{d\tau} &= F^\mu{}_\nu u^\nu + g^\mu,\end{aligned}\tag{2.1}$$

which derivation is quite longish, why we want to refer to literature.

The term  $F^\mu{}_\nu$  describes the electromagnetic field strength tensor

$$F^\mu{}_\nu = \begin{pmatrix} 0 & E_x & E_y & E_z \\ E_x & 0 & B_z & -B_y \\ E_y & -B_z & 0 & B_x \\ E_z & B_y & -B_x & 0 \end{pmatrix}.\tag{2.2}$$

The damping term  $g^\mu$  considers the fact that charged particles radiate fields when they are moving which leads to a loss in their kinetic energy. Within the context of classical electrodynamics Max *Abraham* and Hendrick *Lorentz* discussed radiation damping in their same-named equation first. In 1938 *Dirac* generalized the equation whilst taking special relativity into account.

We now want to deal with how to solve the Lorentz-Newton equation (2.1) numerically.

### 2.2 Euler-Scheme

The most simple method is the explicit *Euler-Method*. It's easy to implement but not very accurate, as we shall see later. But before we go into the details of the explicit Euler-Scheme we need to address some prerequisites all following methods will have in

common.

Starting point will always be a first order system of the kind

$$\begin{aligned}\frac{dx^\mu}{d\tau} &= u^\mu \\ \frac{du^\mu}{d\tau} &= f^\mu(x^\nu, u^\nu) \\ x^\mu(\tau_0) &= x_0^\mu \\ u^\mu(\tau_0) &= u_0^\mu.\end{aligned}\tag{2.3}$$

Systems of higher order can always be reduced to a first order system.

In order to solve the equation of motion numerically the domain needs to be discretized. Therefore we divide the time interval into  $N$  equidistant partial intervals  $h$ , by defining

$$h := \Delta\tau = \tau_{i+1} - \tau_i.$$

The idea is to calculate each point along the trajectory  $x_i^\mu = x^\mu(\tau_i)$  iteratively, starting from the initial values  $x_0^\mu$  and  $u_0^\mu$ . But to calculate these points all differential operators in (2.3) need to be discretized as well. That is where all methods differ. Each method has its own way to discretize the differential operators.

The basis of the Euler-Scheme is a first order Taylor expansion of the integration variable  $x^\mu$  in  $\tau$  around  $\tau_i$

$$x^\mu(\tau_{i+1}) = x^\mu(\tau_i) + \frac{dx^\mu}{d\tau} \Big|_{\tau=\tau_i} \underbrace{(\tau_{i+1} - \tau_i)}_{=h} + \mathcal{O}(h^2).\tag{2.4}$$

Analogously for  $u^\mu$  and solving for  $\frac{dx^\mu}{d\tau}$  and  $\frac{du^\mu}{d\tau}$  respectively yields

$$\begin{aligned}\frac{x_{i+1}^\mu - x_i^\mu}{h} &= u_i^\mu \\ \frac{u_{i+1}^\mu - u_i^\mu}{h} &= f^\mu(x_i^\nu, u_i^\nu).\end{aligned}\tag{2.5}$$

This way of discretizing allows a very easy calculation of  $x_i^\mu$  according to

$$\begin{aligned}x_{i+1}^\mu &= x_i^\mu + h u_i^\mu \\ u_{i+1}^\mu &= u_i^\mu + h f^\mu(x_i^\nu, u_i^\nu).\end{aligned}\tag{2.6}$$

In order for us to calculate the goodness of this approximation we need to introduce the *Procedural Error* and the *Order of Consistency*.<sup>[4]</sup>



### 2.2.1 Procedural Error and Order of Consistency

**Definition 2.2.1 (Procedural Error and Order of Consistency)** Let  $I \subseteq \mathbb{R}$  be a interval,  $f : I \times \mathbb{R}^d \rightarrow \mathbb{R}^d$ ,  $y : I \rightarrow \mathbb{R}^d$  a solution of the initial value problem

$$\begin{aligned} \frac{d}{d\tau} y(\tau) &= f(\tau, y(\tau)), \\ y(\tau_0) &= y_0. \end{aligned} \quad (2.7)$$

(a) The term

$$\eta(\tau, h) := y(\tau) + hf(\tau, y(\tau)) - y(\tau + h) \quad \text{for } \tau \in I, \ 0 < h \leq b - \tau \quad (2.8)$$

is called local Procedural Error of the One-Step-Scheme at  $\tau$  for the increment  $h$ .

(b) The One-Step-Scheme has an Order of Consistency  $p \geq 1$ , if the local Procedural Error fulfils

$$\|\eta(\tau, h)\| \leq Ch^{p+1} \quad \text{for } \tau \in I, \ 0 < h \leq b - \tau, \quad (2.9)$$

with a constant  $C \geq 0$ , which is independent of  $\tau$  and  $h$ .

Descriptively the Procedural Error is the difference between the exact solution  $y(\tau + h)$  and the result, which we get from the One-Step-Scheme starting from the exact solution at the earlier time step  $y(\tau)$ . Figure 2.1 illustrates the situation.

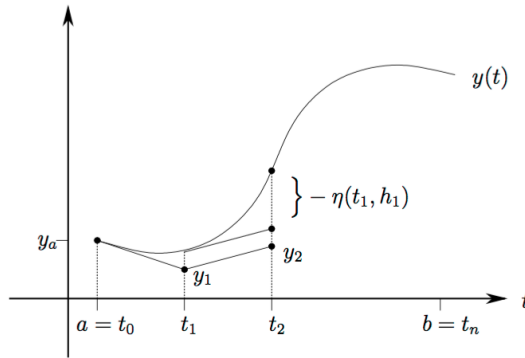


Figure 2.1.: Illustration of the Procedural Errors of an One-Step-Scheme. [4]

We now want to use the definitions 2.2.1 to calculate the Order of Consistency of the Euler-Scheme.

Starting point is the system (2.1). Thereby we focus on the equation for  $u^\mu$ , since  $x^\mu$  can be easily integrated from  $u^\mu$ . Following Definition 2.2.1 we have

$$y = u^\mu. \tag{2.10}$$

We get

$$\eta(\tau, h) = u^\mu(\tau_i) + hf^\mu(x^\nu, u^\nu) - u^\mu(\tau_{i+1}). \tag{2.11}$$

The last term can be calculated with a Taylor-expansion analogously to (2.4).

$$u^\mu(\tau_{i+1}) = u^\mu(\tau_i) + h \left. \frac{du^\mu}{d\tau} \right|_{s=\tau_i} + h^2 \left. \frac{d^2u^\mu}{d\tau^2} \right|_{s=\tau_i}. \tag{2.12}$$

Plugging in (2.12) in (2.11) yields

$$\begin{aligned} \eta(\tau, h) &= u^\mu(\tau_i) + h \frac{du^\mu}{d\tau} - u^\mu(\tau_{i+1}) \\ \stackrel{(2.12)}{\implies} \eta(\tau, h) &= u^\mu(\tau_i) + h \frac{du^\mu}{d\tau} - u^\mu(\tau_i) - h \frac{du^\mu}{d\tau} - h^2 \frac{d^2u^\mu}{d\tau^2} \\ \iff \eta(\tau, h) &= \frac{d^2u^\mu}{d\tau^2} h^2, \end{aligned} \tag{2.13}$$

since  $\frac{du^\mu}{d\tau} = f^\mu(x^\nu, u^\nu)$  holds for the Euler-Scheme. Thus

$$|\eta(\tau, h)| \leq Ch^2 \quad \text{with } C := \frac{1}{2} \max_{\tau \in \mathcal{D}(u^\mu)} \left| \frac{d^2u^\mu}{d\tau^2} \right|. \tag{2.14}$$

$\mathcal{D}(u^\mu)$  denotes the domain of  $u^\mu$ . Therefore, the Euler-Scheme has an Order of Consistency of one.

### 2.3 Leap-Frog-Scheme

A definitely better method is the so called *Leap-Frog*-Scheme. One can easily proof that it has an Order of Consistency of two.

In contrast to the explicit Euler-Scheme this method has several advantages. For one it is time reversible, i.e. it is possible to reach any previous point in time from every point later in the trajectory. On the other hand the Leap-Frog-Scheme is symplectic, meaning

it conserves the phase space volume from which energy and momentum conservation follows.

However, one disadvantage is that it's only suited for systems in which the acting force exclusively depends on the current position, but not on the velocity of the particle. This would lead to an implicit equation system which is numerically way more expensive to solve.

Thus the differential equation should be of the form

$$\frac{d^2 x^\mu}{d\tau^2} = \frac{du^\mu}{d\tau} = f^\mu(x^\nu). \quad (2.15)$$

As we already mentioned, the various methods discretize the differential operators differently. The Leap-Frog-Scheme uses

$$\begin{aligned} \frac{x_{i+1}^\mu - x_i^\mu}{h} &= u_{i+\frac{1}{2}}^\mu \\ \frac{u_{i+\frac{1}{2}}^\mu - u_{i-\frac{1}{2}}^\mu}{h} &= f^\mu(x_i^\nu). \end{aligned} \quad (2.16)$$

Solving for the new time step yields

$$\begin{aligned} x_{i+1}^\mu &= x_i^\mu + h u_{i+\frac{1}{2}}^\mu \\ u_{i+\frac{1}{2}}^\mu &= u_{i-\frac{1}{2}}^\mu + h f^\mu(x_i^\nu). \end{aligned} \quad (2.17)$$

As we can see, position and velocity are calculated at different times. They are shifted against each other in time by  $h = \frac{1}{2}$ .

But what if we have a system in which the force depends on the velocity? Are we stuck with expensive implicit methods? Fortunately not. We can use the *Boris* - Method.

### 2.3.1 Boris-Method

This method was invented in 1970 by J.P. Boris<sup>[2]</sup> and is the standard method for pushing particles in plasma simulations today. We want to solve the Lorentz-Newton equation

$$\frac{v_{i+\frac{1}{2}} - v_{i-\frac{1}{2}}}{h} = \frac{q}{m} \left( \vec{E} + \frac{v_{i+\frac{1}{2}} + v_{i-\frac{1}{2}}}{2} \times \vec{B} \right) \quad (2.18)$$

Boris noticed, that upon defining

$$\begin{aligned} \vec{v}_- &:= v_{i-\frac{1}{2}} + \frac{h q \vec{E}}{2 m} \quad \text{and} \\ \vec{v}_+ &:= v_{i+\frac{1}{2}} + \frac{h q \vec{E}}{2 m}, \end{aligned} \quad (2.19)$$

one can eliminate the electric field. Plugging in (2.19) into (2.18) yields

$$\frac{\vec{v}_+ - \vec{v}_-}{h} = \frac{q}{m}(\vec{v}_+ + \vec{v}_-) \times \vec{B}. \quad (2.20)$$

Following the geometrical analysis in [3] we find

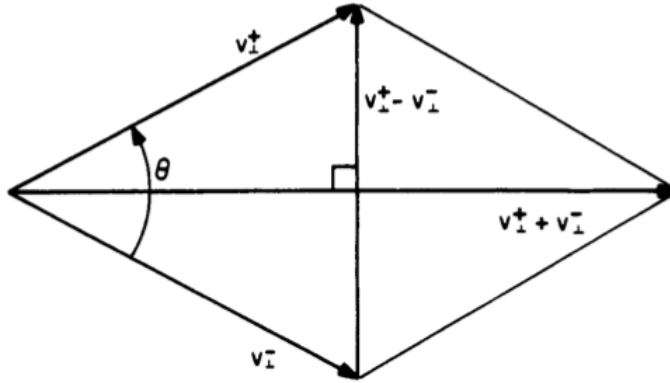


Figure 2.2.: Blah Blah

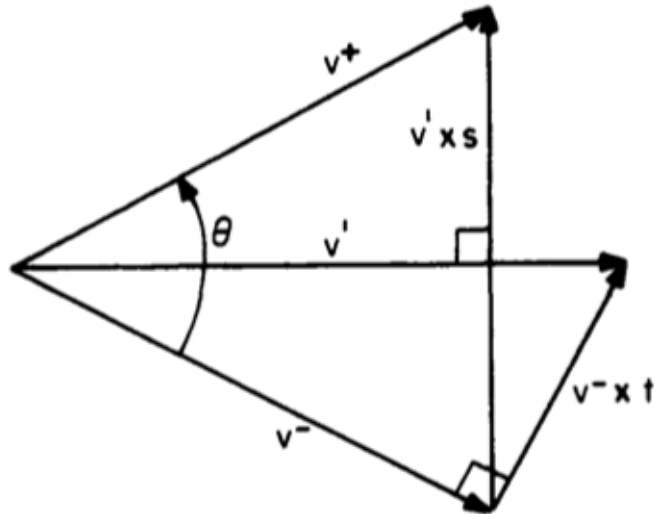


Figure 2.3.: Blah Blah

## 2.4 Nyström-Scheme

## 2.5 Adaptive Timestep Control

---

## Interpolations

---

### 3.1 Linear interpolation of Trajectories

The previously presented methods calculate the particle trajectory solely at discrete points in time  $x_i^\mu(\tau)$ . Calculating Liénard-Wiechert fields according to equation (1.32) however, requires the intersection point of the trajectory with the backward lightcone of the observation point. In most cases the calculated points of the trajectory are not lying directly on the lightcone, so we need a procedure to calculate the intersection point exactly.

The simplest solution is a linear interpolation between the last point inside and the first point outside the lightcone. Figure 3.1 illustrates the situation.

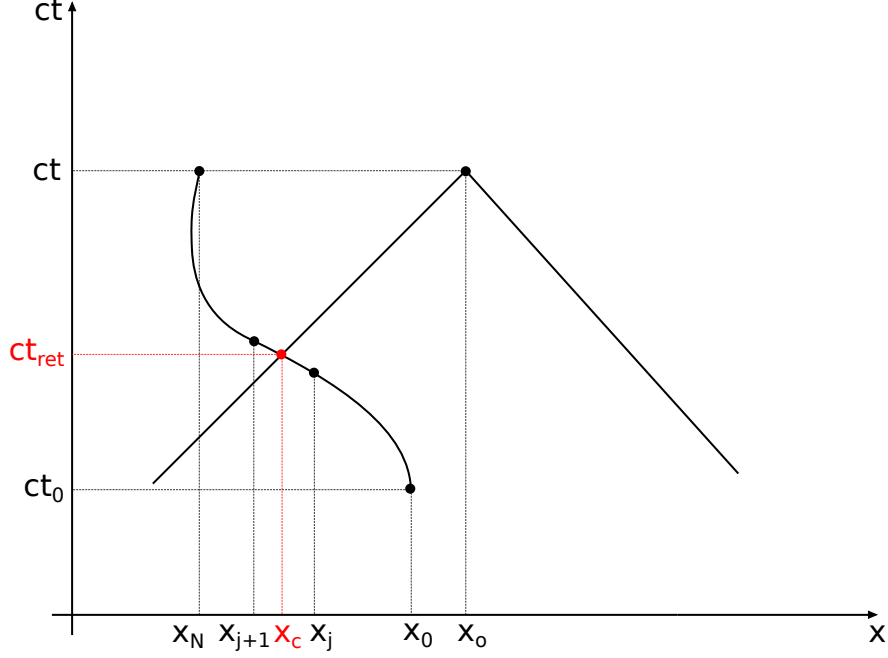


Figure 3.1.: Minkowski space showing the particle trajectory with starting point  $x_0^\mu(t_0)$  and last point  $x_N^\mu(t)$ . The observation point  $x_o^\mu(t)$  with its backward lightcone is also shown. If we want to calculate the Liénard-Wiechert fields at the observation point  $x_o^\mu(t)$ , we need the intersection point  $x_c^\mu(t_{ret})$  of the trajectory with the backward lightcone.

There to let  $x_j^\mu \in \mathbb{R}^{3+1}$  be the last point inside and  $x_{j+1}^\mu \in \mathbb{R}^{3+1}$  the first point outside the lightcone. Further let  $x_c^\mu \in \mathbb{R}^{3+1}$  be the intersection point of interest then we get

$$x_c^\mu = x_j^\mu + \lambda \left( x_{j+1}^\mu - x_j^\mu \right), \quad (3.1)$$

where  $\lambda \in [0, 1]$ . Due to the finite speed of light the intersection point  $x_c^\mu$  needs to fulfill

$$|\vec{x}_o(t) - \vec{x}_c(t_{ret})| = c (t - t_{ret}) \iff (x_o - x_c)_\mu (x_o - x_c)^\mu = 0. \quad (3.2)$$

Thereby  $x_o^\mu \in \mathbb{R}^{3+1}$  denotes the observation point where the fields shall be calculated. Note, that on the left hand side of (3.2) only spatial components of the respective four vectors are used.

Plugging in (3.1) in (3.2) yields

$$\lambda^2(x_{j+1} - x_j)_\mu(x_{j+1} - x_j)^\mu + \lambda 2(x_{j+1} - x_j)_\mu(x_j - x_o)^\mu + (x_j)_\mu(x_j)^\mu + (x_o)_\mu(x_o)^\mu - 2(x_j)_\mu(x_o)^\mu = 0. \quad (3.3)$$

We define

$$\begin{aligned} a &:= (x_{j+1} - x_j)_\mu(x_{j+1} - x_j)^\mu \\ b &:= 2(x_{j+1} - x_j)_\mu(x_j - x_o)^\mu \\ c &:= (x_j)_\mu(x_j)^\mu + (x_o)_\mu(x_o)^\mu - 2(x_j)_\mu(x_o)^\mu. \end{aligned}$$

In general the quadratic equation (3.3) in  $\lambda$  has two solutions

$$\lambda_{1/2} = \frac{-b \pm \sqrt{b^2 - 4ac}}{2a}.$$

One denotes the intersection point with the backward lightcone, the other one with the forward lightcone. Since  $\lambda \in [0, 1]$  we are only interested in the larger one.

$$\lambda_{1/2} = \frac{-b + \sqrt{b^2 - 4ac}}{2a}.$$

Plugging in  $\lambda$  in (3.1) gives the desired intersection point.

## 3.2 Trilinear Interpolation of Fields



---

## FDTD

---

In this section we introduce the concept of hybrid fields and how this approach reduces the numerical complexity from  $N^2$  to  $N$ .

Usually the numerical complexity of multi particle simulation is  $N^2$ , due to the interaction between each particle. In our case we need  $N$  push operations for the particles. One push for each particle. In order to do that, however, we need to solve equation (2.1) and therefore all Liénard-Wiechert fields from the other  $N - 1$  particles are needed. This results in  $N(N - 1)$  calculations for each time step, period. If we want to calculate the Liénard-Wiechert fields, we also need to store all positions from all particles, as explained in section 3.1. For a few particles such simulations are effortlessly feasible. But with increasing particle numbers such simulations may not just require more and more memory capacity but also become so time consuming that at some point we simply can not do them anylonger. That's where the hybrid field model comes in. Instead of calculating the Liénard-Wiechert fields at every time step for all particles at all grid points we save them onto the grid and propagate them through the grid using Maxwell equations. How that works in detail is explained in the following sections.

### 4.1 Maxwell-Equations

The Maxwell equations are the foundation of the classical electromagnetism and describe how the electric field  $\vec{E} \in \mathbb{R}^3$  and the magnetic field  $\vec{H} \in \mathbb{R}^3$  are generated by charges and currents respectively and how they evolve over time in space in presence of one another. In homogenous and isotropic media the Maxwell Equations read

$$\begin{aligned}
 \epsilon_0 \epsilon_r \vec{\nabla} \cdot \vec{E} &= \rho \\
 \mu_0 \mu_r \vec{\nabla} \cdot \vec{B} &= 0 \\
 \vec{\nabla} \times \vec{E} &= -\mu_0 \mu_r \frac{\partial \vec{B}}{\partial t} \\
 \vec{\nabla} \times \vec{H} &= \epsilon_0 \epsilon_r \frac{\partial \vec{E}}{\partial t} + \sigma \vec{E},
 \end{aligned} \tag{4.1}$$

where  $\epsilon_0$  and  $\epsilon_r$  are the vacuum and the relative electric permeability respectively. Same holds for  $\mu_0$  and  $\mu_r$  for magnetic materials.  $\rho$  denotes the current density of the electric source and  $\sigma$  the electric conductivity.

To solve the Maxwell equations numerically we need to discretize them first. The most robust and reliable way of doing this is with the *Yee-Algorithm*.

## 4.2 The Yee-Scheme

In this section we talk about how to solve the Maxwell Equations (4.1) and how to propagate the fields on a numerical grid. We thereby focus on the Maxwell Equations in vacuum, i.e.  $\rho = \sigma = 0$  and  $\epsilon_r = \mu_r = 1$ . As can be seen in the Liénard-Wiechert formula (1.32) there is a singularity for the field values at the particle position itself. Thus, we just want to propagate fields far away from the source, which is explained in more detail later.

To push the fields on the grid. i.e solving for the fields at the next time step, we use the Yee - Scheme introduced by *Kane Yee* in 1966.<sup>[7]</sup>

Figure 4.1 illustrates a so called Yee-Box and the components we need to solve the curl equations of (4.1).

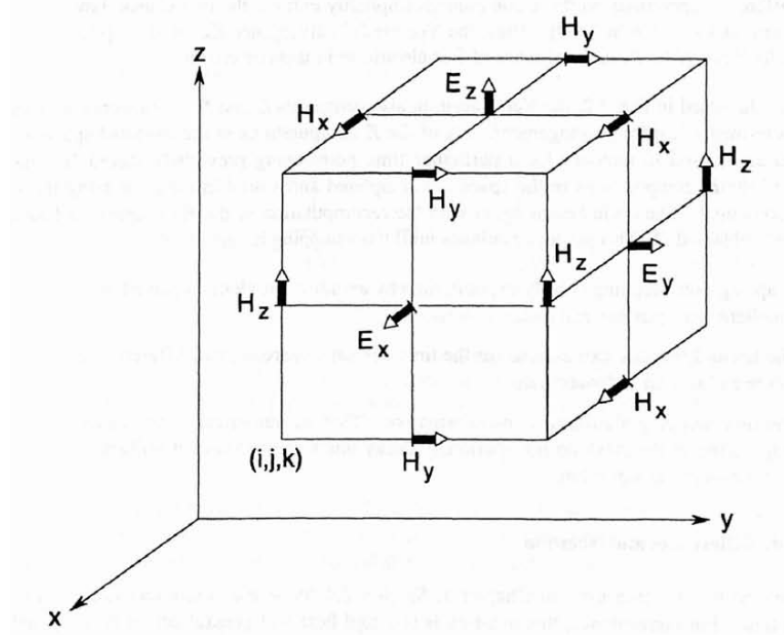


Figure 4.1.: An illustration of a Yee-Box which is used to solve the curl Maxwell Equations. Shown are the positions of the electric and magnetic field vector components about a cubic unit cell of the Yee space lattice. The Yee algorithm centers its E and H components in three-dimensional space so that every E component is surrounded by four circulating H components, and every H component is surrounded by four circulating E components.<sup>[6]</sup>

### 4.3 Numeric Dispersion Relation

---

## Hybrid Field Approach

---

- 5.1 Near-and Farfields
- 5.2 Particle Push and Nearfield Update
- 5.3 Particle History
- 5.4 Farfield Setup Before Simulation
- 5.5 Electron Scattering in an electromagnetic wave

---

## Uniaxial Perfectly Matched Layer

---

Part III.

Summary

Part IV.

Appendix

---

## Gauge Transformations

---

In this chapter we want to show, that the gauge fields leave both the electric and magnetic fields and the corresponding potential equations invariant.

### A.1 Invariance of Fields

We want to show that  $\vec{E}' = \vec{E}$  and  $\vec{B}' = \vec{B}$ .

$$\begin{aligned}
 \vec{E}' &= -\vec{\nabla}\varphi' - \frac{\partial \vec{A}'}{\partial t} \\
 &= -\vec{\nabla}\left(\varphi - \frac{\partial\psi}{\partial t}\right) - \frac{\partial}{\partial t}\left(\vec{A} + \vec{\nabla}\psi\right) \\
 &= -\vec{\nabla}\varphi + \vec{\nabla}\left(\frac{\partial\psi}{\partial t}\right) - \frac{\partial \vec{A}}{\partial t} - \frac{\partial}{\partial t}(\vec{\nabla}\psi) \\
 &= \vec{E}
 \end{aligned}$$

and

$$\begin{aligned}
 \vec{B}' &= \vec{\nabla} \times \vec{A}' \\
 &= \vec{\nabla} \times \left(\vec{A} + \vec{\nabla}\psi\right) \\
 &= \vec{\nabla} \times \vec{A} + \vec{\nabla} \times (\vec{\nabla}\psi) \\
 &= \vec{B}.
 \end{aligned}$$



## A.2 Invariance of Potential Equations

Now we want to show the invariance of the potential equations. Therefore consider

$$\begin{aligned}
 & -\Delta\varphi' - \vec{\nabla} \left( \frac{\partial \vec{A}'}{\partial t} \right) = \frac{\rho}{\epsilon_0} \\
 \iff & -\Delta \left( \varphi - \frac{\partial \psi}{\partial t} \right) - \vec{\nabla} \left[ \frac{\partial}{\partial t} (\vec{A} + \vec{\nabla} \psi) \right] = \frac{\rho}{\epsilon_0} \\
 \iff & -\Delta\varphi + \Delta \left( \frac{\partial \psi}{\partial t} \right) - \vec{\nabla} \left( \frac{\partial \vec{A}}{\partial t} \right) - \vec{\nabla} \left[ \frac{\partial}{\partial t} (\vec{\nabla} \psi) \right] = \frac{\rho}{\epsilon_0} \\
 \iff & -\Delta\varphi - \vec{\nabla} \left( \frac{\partial \vec{A}}{\partial t} \right) = \frac{\rho}{\epsilon_0}
 \end{aligned}$$

and

$$\begin{aligned}
 & \square \vec{A}' - \vec{\nabla} \left( \vec{\nabla} \vec{A}' + \frac{1}{c^2} \frac{\partial \varphi'}{\partial t} \right) = -\mu_0 \vec{j} \\
 \iff & \hat{\square} (\vec{A} + \vec{\nabla} \psi) - \vec{\nabla} \left[ \vec{\nabla} (\vec{A} + \vec{\nabla} \psi) + \frac{1}{c^2} \frac{\partial}{\partial t} \left( \varphi - \frac{\partial \psi}{\partial t} \right) \right] = -\mu_0 \vec{j} \\
 \iff & \hat{\square} \vec{A} + \square (\vec{\nabla} \psi) - \vec{\nabla} \left[ \vec{\nabla} \vec{A} + \Delta \psi + \frac{1}{c^2} \frac{\partial \varphi}{\partial t} - \frac{1}{c^2} \frac{\partial^2 \psi}{\partial t^2} \right] = -\mu_0 \vec{j} \\
 \iff & \hat{\square} \vec{A} + \square (\vec{\nabla} \psi) - \vec{\nabla} \left[ \vec{\nabla} \vec{A} + \square \psi + \frac{1}{c^2} \frac{\partial \varphi}{\partial t} \right] = -\mu_0 \vec{j} \\
 \iff & \hat{\square} \vec{A} - \vec{\nabla} \left( \vec{\nabla} \vec{A} + \frac{1}{c^2} \frac{\partial \varphi}{\partial t} \right) = -\mu_0 \vec{j}
 \end{aligned}$$

## Retarded Potential Equations Fulfill Laurentz Gauge

We show that the retarded potential equations

$$\begin{aligned}\varphi(\vec{r}, t) &= \frac{1}{4\pi\epsilon_0} \int_V \frac{\rho(\vec{r}', t_{ret})}{|\vec{r} - \vec{r}'|} d\vec{r}', \\ \vec{A}(\vec{r}, t) &= \frac{\mu_0}{4\pi} \int_V \frac{\vec{j}(\vec{r}', t_{ret})}{|\vec{r} - \vec{r}'|} d\vec{r}'\end{aligned}$$

with  $t_{ret} := t - \frac{|\vec{r} - \vec{r}'|}{c}$  fulfill the Laurentz Gauge

$$\vec{\nabla} \vec{A} + \frac{1}{c^2} \frac{\partial \varphi}{\partial t} = 0.$$

Plugging in yields

$$\begin{aligned}\vec{\nabla} \vec{A} + \frac{1}{c^2} \frac{\partial \varphi}{\partial t} &= \frac{\mu_0}{4\pi} \int_V \vec{\nabla}_{\vec{r}} \frac{\vec{j}(\vec{r}', t_{ret})}{|\vec{r} - \vec{r}'|} d\vec{r}' + \frac{1}{c^2} \frac{1}{4\pi\epsilon_0} \int_V \frac{\partial}{\partial t} \frac{\rho(\vec{r}', t_{ret})}{|\vec{r} - \vec{r}'|} d\vec{r}' \\ &= \frac{\mu_0}{4\pi} \int_V \vec{\nabla}_{\vec{r}} \frac{\vec{j}(\vec{r}', t_{ret})}{|\vec{r} - \vec{r}'|} \frac{\partial}{\partial t} \frac{\rho(\vec{r}', t_{ret})}{|\vec{r} - \vec{r}'|} d\vec{r}',\end{aligned}$$

where we used  $c^2 = \frac{1}{\mu_0\epsilon_0}$ . Now consider the first term in the integrand

$$\begin{aligned}\vec{\nabla}_{\vec{r}} \frac{\vec{j}(\vec{r}', t_{ret})}{|\vec{r} - \vec{r}'|} &= \vec{j}(\vec{r}', t_{ret}) \vec{\nabla}_{\vec{r}} \left( \frac{1}{|\vec{r} - \vec{r}'|} \right) + \frac{1}{|\vec{r} - \vec{r}'|} \partial_{t_{ret}} \vec{j}(\vec{r}', t_{ret}) \vec{\nabla}_{\vec{r}} t_{ret} \\ &= -\vec{j}(\vec{r}', t_{ret}) \frac{\vec{r} - \vec{r}'}{|\vec{r} - \vec{r}'|^3} - \frac{1}{c} \frac{\vec{r} - \vec{r}'}{|\vec{r} - \vec{r}'|^2} \partial_{t_{ret}} \vec{j}(\vec{r}', t_{ret})\end{aligned}$$

On the other hand we also have

$$\begin{aligned}\vec{\nabla}_{\vec{r}'} \frac{\vec{j}(\vec{r}', t_{ret})}{|\vec{r} - \vec{r}'|} &= \vec{j}(\vec{r}', t_{ret}) \vec{\nabla}_{\vec{r}'} \left( \frac{1}{|\vec{r} - \vec{r}'|} \right) + \frac{1}{|\vec{r} - \vec{r}'|} \left( \vec{\nabla}_{\vec{r}'} \vec{j}(\vec{r}', t_{ret}) \Big|_{t_{ret}} + \partial_{t_{ret}} \vec{j}(\vec{r}', t_{ret}) \vec{\nabla}_{\vec{r}'} t_{ret} \right) \\ &= \vec{j}(\vec{r}', t_{ret}) \frac{\vec{r} - \vec{r}'}{|\vec{r} - \vec{r}'|^3} + \frac{1}{|\vec{r} - \vec{r}'|} \left( \vec{\nabla}_{\vec{r}'} \vec{j}(\vec{r}', t_{ret}) \Big|_{t_{ret}} + \frac{1}{c} \frac{\vec{r} - \vec{r}'}{|\vec{r} - \vec{r}'|} \partial_{t_{ret}} \vec{j}(\vec{r}', t_{ret}) \right),\end{aligned}$$

APPENDIX B. RETARDED POTENTIAL EQUATIONS FULFILL  
LAURENTZ GAUGE

---

which means that we can write

$$\vec{\nabla}_{\vec{r}} \frac{\vec{j}(\vec{r}', t_{ret})}{|\vec{r} - \vec{r}'|} + \vec{\nabla}_{\vec{r}'} \frac{\vec{j}(\vec{r}', t_{ret})}{|\vec{r} - \vec{r}'|} = \frac{\vec{\nabla}_{\vec{r}'} \vec{j}(\vec{r}', t_{ret}) \Big|_{t_{ret}}}{|\vec{r} - \vec{r}'|}.$$

Plugging in this into (B.1) yields

$$\vec{\nabla} \vec{A} + \frac{1}{c^2} \frac{\partial \varphi}{\partial t} = \frac{\mu_0}{4\pi} \int_V -\vec{\nabla}_{\vec{r}'} \frac{\vec{j}(\vec{r}', t_{ret})}{|\vec{r} - \vec{r}'|} + \underbrace{\frac{\vec{\nabla}_{\vec{r}'} \vec{j}(\vec{r}', t_{ret}) \Big|_{t_{ret}}}{|\vec{r} - \vec{r}'|} + \frac{\partial}{\partial t} \frac{\rho(\vec{r}', t_{ret})}{|\vec{r} - \vec{r}'|}}_{=0 \text{ due to continuity equation}} d\vec{r}'.$$

For the remaining first term we use *Stokes Law*

$$\vec{\nabla} \vec{A} + \frac{1}{c^2} \frac{\partial \varphi}{\partial t} = -\frac{\mu_0}{4\pi} \int_V \vec{\nabla}_{\vec{r}'} \frac{\vec{j}(\vec{r}', t_{ret})}{|\vec{r} - \vec{r}'|} d\vec{r}' = -\frac{\mu_0}{4\pi} \oint_{\partial V} \frac{\vec{j}(\vec{r}', t_{ret})}{|\vec{r} - \vec{r}'|} d\vec{\sigma} = 0,$$

because the current density vanishes at infinity. That's what we wanted to show.

---

## Softwarestack

---

---

## Code Documentation

---

---

## Normalization

---

---

## List of Figures

---

1.1. Illustration of how to calculate the energy emission of a moving particle with charge $q$ . . . . .	10
1.2. Radiation characteristics of an moving charged particle . . . . .	13
2.1. Procedural Error . . . . .	18
2.2. Caption . . . . .	21
2.3. Caption . . . . .	22
3.1. Interpolation of Trajectories . . . . .	24
4.1. Yee-Box . . . . .	28

---

## Bibliography

---

- [1] M. P. Allen and D. J. Tildesley. *Computer Simulation of Liquids*. Clarendon Press, New York, NY, USA, 1989.
- [2] J. P. Boris. Relativistic plasma simulation-optimization of a hybrid code. *Proceeding of Fourth Conference on Numerical Simulations of Plasmas*, November 1970.
- [3] A. Bruce Langdon Charles K. Birdsall. *Plasma physics via computer simulation*. IOP, 1991.
- [4] Christian Kanzow. *Numerische Mathematik II*. 2005. [Online; accessed 13-Oktober-2016].
- [5] W. Nolting. *Grundkurs Theoretische Physik 3:.* Grundkurs Theoretische Physik / Wolfgang Nolting. Springer, 2004.
- [6] A. Taflov and S.C. Hagness. *Computational Electrodynamics: The Finite-difference Time-domain Method*. Artech House antennas and propagation library. Artech House, 2005.
- [7] Kane S. Yee. Numerical solution of initial boundary value problems involving maxwell's equations in isotropic media. *IEEE Trans. Antennas and Propagation*, pages 302–307, 1966.



---

## Declaration

---

Erklärung:

Hiermit erkläre ich, die vorliegende Arbeit selbständig verfasst zu haben und keine anderen als die in der Arbeit angegebenen Quellen und Hilfsmittel benutzt zu haben.

München, Datum der Abgabe

---

München, 18.07.2017, David Symhoven